https://doi.org/10.5194/egusphere-2025-3670
Preprint. Discussion started: 19 September 2025

Atmospheric blocking and climate extremes in Germany in present and future climate

Richard Lohmann[1], Christopher Purr[1,2], and Bodo Ahrens[1]

[1]Institute for Atmospheric and Environmental Sciences; Goethe University, Frankfurt, Germany
[2]Current address: Deutscher Wetterdienst (DWD), Offenbach, Germany

Correspondence: Richard Lohmann (Lohmann@iau.uni-frankfurt.de)

Abstract. Atmospheric blocking is linked to extreme weather and climate events like heatwaves, heavy rainfall, and calm weather. The statistical relationship between blocking and extreme events in Germany is quantified in atmospheric reanalyses ERA5, ERA-20C, and 20CRv3, and in historical and future CMIP6 climate simulations. This targets the reliability assessment of climate projections regarding extreme events in the 21st century. The analysis of the atmospheric reanalyses in the period 1961-2010 indicates that days with blocking see heatwaves 10-11 times and heavy precipitation events or calms 1.5 to 3 times more often than days without blocking. These empirical relationships are also seen in historical CMIP6 simulations for the large-scale phenomena heatwaves and calms, but not for heavy precipitation events (with odds only 1-1.5 times higher given a day with blocking than without). In the simulated future climate, the relationship of blocking with the three extreme event types changes only moderately. Inconsistent blocking trends in the projections, particularly in summer, obstruct the robust projection of extreme events in Germany despite the stable relationship between blocking and heatwaves and calms in most of the CMIP6 simulations. Furthermore, the results confirm the need for better representation of precipitation extremes in climate models.

1 Introduction

Weather and climate extremes have a high socio-economic impact. Most of these extremes pertain to three categories: temperature extremes (heatwave/cold spell), hydrological extremes (flood/drought), and wind extremes (storm/calm) (Kron et al., 2019). In Europe, floods cause the highest economic loss of all natural hazards (Raška, 2015), whereas heatwaves are the deadliest events, linked to several thousand fatalities per event (Kovats and Kristie, 2006; Kautz et al., 2022). Prominent examples of deadly heatwaves in Europe are the 2003 heatwave with 70,000 heat-related fatalities and the 2010 heatwave with 55,000 fatalities (Barriopedro et al., 2011). Prominent examples of severe floods with high economical damage are the Central European floods in 2002 (14.5 billion EUR), 2013 (11 billion EUR) or 2021 (46 billion EUR) (Blöschl et al., 2013; Kron et al., 2019; Kautz et al., 2022; Tradowsky et al., 2023). Examples for storms in Europe are Daria (1990), Lothar (1999), and Kyrill (2007) (Kron et al., 2019). Periods of weak winds (hereafter called calms) do not have such a high impact as storms. However, they have relevance for renewable energy production, especially in winter when energy production by solar power is low (Drücke et al., 2021; Mockert et al., 2023).

https://doi.org/10.5194/egusphere-2025-3670
Preprint. Discussion started: 19 September 2025

The commonality of many extreme events is their link to a phenomenon called atmospheric blocking (hereafter: blocking). Blocking is a mid- to high-latitude phenomenon characterised by a persistent high-pressure system with a lifetime of up to several weeks (Woollings et al., 2018). A typical feature is the diversion or disruption of the typical westerly flow (i.e. the flow is more meridional than zonal in and around the area of a high-pressure system) (Rex, 1950; Kautz et al., 2022). The persistence of these high-pressure systems can cause extreme weather events. Inside the block, subsiding air favours clear sky conditions. The resulting solar insolation, in combination with adiabatic warming of subsiding air, causes heatwaves in summer (Pfahl and Wernli, 2012; Pfahl, 2014; Woollings et al., 2018; Kautz et al., 2022). These are intensified by the dry weather condition in persistent blocks which reduces the soil moisture and increases the Bowen ratio (Fischer et al., 2007; Pfahl and Wernli, 2012; Pfahl, 2014). In winter, clear sky conditions favour the cooling of the lower troposphere. However, advection of cold air at the eastern and southern flank of the block is the dominant driver of cold spells (Cattiaux et al., 2010; Sousa et al., 2018; Woollings et al., 2018; Kautz et al., 2022). Advection of warm air at the northwestern flank of the high-pressure system is the dominant driver of winter heatwaves (Holmberg et al., 2023). On the other hand, intense precipitation and floods are observed more frequently at the southwestern and southeastern flank of the block than without blocking (Sousa et al., 2017; Lenggenhager and Martius, 2019). Furthermore, blocking modifies the occurrence of wind extremes. First, blocking changes the storm tracks, e.g. southward to the Mediterranean in the case of Greenland blocking. Second, a surface high-pressure system corresponding to the block in the mid-troposphere increases the surface pressure gradient, if well pronounced, resulting in enhanced winds between high- and low-pressure system (Pfahl, 2014; Kautz et al., 2022). Concurrently, weak winds dominate in the centre of the high-pressure system (Grams et al., 2017; Drücke et al., 2021; Mockert et al., 2023).

For the future climate, climate models simulate an increase in the number and intensity of heatwaves and precipitation extremes (Russo et al., 2014; Blöschl et al., 2020; Lin et al., 2022; Stanley et al., 2023). However, the degree of change is uncertain, especially for high-emission scenarios (Russo et al., 2014; Huo et al., 2021; Stanley et al., 2023), since the spread of, e.g., frequency of heatwaves in climate simulations scales with the global warming level (Barriopedro et al., 2023). The uncertainty in the number and intensity of future extreme events is enhanced by uncertainties in the frequency of future blocking which are described in Davini and D'Andrea (2020) and Lohmann et al. (2024).

Further sources of uncertainty are the representation of the links between blocking and extreme events in climate simulations and a potential change of those links in the future climate. Sillmann and Croci-Maspoli (2009), Sillmann et al. (2011) and Brunner et al. (2018) compared the results between reanalyses and climate simulations and found reasonable agreements. However, they investigated only single models (ECHAM5 in Sillmann and Croci-Maspoli (2009) and Sillmann et al. (2011), and CanESM2 in Brunner et al. (2018)). Thus, we investigate the link between blocking and extreme events in Germany in an ensemble of six climate simulations participating in the *Coupled Model Intercomparison Project Phase 6* (CMIP6) (Eyring et al., 2016) to increase the robustness of the results. The investigation has three steps: First, we quantify the link between blocking and the weather and climate extremes focusing on heatwaves, heavy precipitation events, and calms in three atmospheric reanalyses (i.e. in near-observation datasets). Second, we do the same for CMIP6 simulations and compare the results to the reanalyses. Third, we compare the link between blocking and extreme events between historical and future periods assuming the highest CMIP6 emission scenario SSP5-8.5. The paper is structured as follows: In section 2, we present

https://doi.org/10.5194/egusphere-2025-3670
Preprint. Discussion started: 19 September 2025

the applied data and methods, followed by the results in section 3. In section 4, we discuss the results before we end up with the conclusions in section 5.

2 Data and methods

We compared the statistical link between blocking and extreme events between three reanalyses and six CMIP6 simulations (Eyring et al., 2016). The reanalyses are ERA-20C (Poli et al., 2016), NOAA-CIRES-DOE Twentieth Century Reanalysis v3 (hereafter 20CR) (Slivinski et al., 2019), and ERA5 (Hersbach et al., 2019). The climate simulations are a sub-set of CMIP6 simulations (CESM2, CNRM-CM6-1, MIROC-ES2L, MPI-ESM1-2-HR, NorESM2-MM, UKESM1-0-LL) whose seasonal blocking trends agreed best to the 20CR reanalysis during the period 1900-2014 as described in Lohmann et al. (2024). We analysed the reanalyses and CMIP6 Simulations for the period 1961-2010. For the future, we considered the period 2051-2100 assuming the highest emission scenario SSP5-8.5.

2.1 Extreme events

In the following paragraphs, we define the extremes which we related to blocking. The definitions of the extremes were based on percentiles. This minimises the impact of elevation, geographical position, or spatial resolution on the identification of extreme events. The reference period for the percentile calculation was 1981-2010. The spatial resolution depends on the analysed dataset. ERA-20C and 20CR data have a spatial resolution of $1°$, whereas ERA5 data have a spatial resolution of $0.25°$. The horizontal resolution of the climate models differs and is not a multiple of 0.25 or $1°$. Therefore, when analysing extremes in the climate simulations, the closest grid point in the climate simulations to the investigated grid point in the reanalyses was analysed.

2.1.1 Heatwaves

Following Zampieri et al. (2017) who adapted the method by Russo et al. (2015), heatwaves are periods of at least three subsequent days with a daily maximum temperature above the 90th percentile value (T_{90} percentiles were determined using centered 31-day windows). Furthermore, a daily magnitude M_d considering the temperature anomaly is calculated: The calculation of the magnitude is based on the 25th and 75th percentiles of the daily maximum temperature using centered 31-day windows (T_{25} and T_{75}):

$$M_d(T) = (T - T_{25})/(T_{75} - T_{25}) \quad if\ T > T_{90};\ 0\ otherwise. \tag{1}$$

Zampieri et al. (2017) modified the method by Russo et al. (2015) because Russo et al. (2015) calculated T_{25} and T_{75} with respect to the yearly maximum temperature. The original method by Russo et al. (2015) enables only the calculation of the daily magnitude of summer heatwaves. The sum of M_d over all heatwave days is the magnitude of the heatwave (hereafter called HWMD). We implemented the modification by Zampieri et al. (2017) in the original R code by Russo et al. (2015) which is available in the extRemes package (R Core Team, 2024).

https://doi.org/10.5194/egusphere-2025-3670
Preprint. Discussion started: 19 September 2025

As we expected seasonally varying mechanisms behind the occurrence of heatwaves, we investigated the link between blocking and heatwaves separately for summer (April-September) and winter (October-March) half-years. We analysed heatwaves in general and strong heatwaves and defined strong heatwaves as heatwaves with HWMD>15. Heatwaves were determined at a grid point in Central Germany (51° N, 10° E) representing Germany.

2.1.2 Heavy precipitation

Heavy precipitation events were defined as days with daily precipitation exceeding the 99th percentile value (the percentile calculation includes dry days). Hofstätter et al. (2018) found differences between weather regime climatologies related to heavy precipitation in several parts of Central Europe: heavy precipitation in Northern and Western Germany was predominantly related to Atlantic winter cyclones (no blocking), whereas heavy precipitation over Eastern Germany, Austria and the Czech Republic was predominantly observed in the summer half-year and related to so-called Vb cyclones (potentially with blocking (Grams et al., 2014; Hofstätter et al., 2018)). Therefore, we calculated the link between blocking and heavy precipitation separately for the summer and winter half-year. Furthermore, we distinguished between heavy precipitation at grid points in Western (51° N, 8° E) and Eastern Germany (51° N, 14° E).

2.1.3 Calms

Calm days (hereafter called calms) were defined as days with a daily mean wind speed below the 5th percentile value at 10 m altitude. The wind speed at 100 m height would be more appropriate for calm consideration, but was not available in the 20CR and CMIP6 datasets. The 10 m 5th percentile is an appropriate reference value because for that the wind speed at 100 m height is typically around 2.5 m s^{-1} in Central Germany in ERA5. This wind speed is within the range of the cut-in wind speed (i.e. the minimum wind speed required for wind turbines to produce energy) of many power plants (Enercon, 2025). As for heatwaves, we analysed calms at a grid point in Central Germany (51° N, 10° E). We quantified the empirical link between blocking and calms for the summer and winter half-year. The focus was on the latter period because of relatively low solar energy production and high energy demand (e.g. for heating).

2.2 Blocking

The applied hybrid blocking index evaluates the geopotential height at 500 hPa. This hybrid index combines the gradient approach by Davini et al. (2012) with an anomaly approach based on Barriopedro et al. (2010) which we adapted as described in Lohmann et al. (2024): in case of blocking the geopotential height has to exceed the climatological mean by one standard deviation. The mean value and standard deviation were calculated for each calendar day and grid cell. A 91-day window centered around the day of interest was applied for the calculation of the mean and standard deviation to smooth the yearly cycle. The climatological mean of geopotential height refers to a 31-year running window to consider the increase in the mean geopotential height related to the increase in global mean temperature.

https://doi.org/10.5194/egusphere-2025-3670
Preprint. Discussion started: 19 September 2025

In the first step, both components of the hybrid index were calculated independently. To combine both, blocked areas were checked for an overlap of at least $1.5 \cdot 10^5$ km^2. If this area was achieved, the full area detected by the anomaly approach was counted as instantaneous block. Next, a spatio-temporal filtering was applied. The instantaneous block was finally counted as block if the block persists for at least five days, covers at least 15° in longitude and $1.5 \cdot 10^6$ km^2 in space. The advantage of the hybrid index is that it captures the full spatial extent of the high-pressure system which is favourable for investigating the link between blocking and extreme events. We calculated the blocking data with the 2D-Blocking Plugin (Richling, 2020) which is part of the Free Evaluation System Framework (Freva) (Kadow et al., 2021). The geopotential height fields of all datasets were remapped to a 2.5°x2.5° grid, since this spatial resolution is the default setting of the 2D-Blocking Plugin (Richling, 2020).

2.3 Relating blocking to extreme events

The first step was to identify areas with blocking which are empirically linked to extreme event time series at the selected locations in Germany. For this purpose, two conditional frequencies were calculated at each blocking grid cell: first, the frequency of blocking during an extreme event $f_{block|ext}$ which is the percentage of blocking at a grid cell given an extreme event at the selected location in Germany. Second, the frequency of an extreme event during blocking $f_{ext|block}$ which is the percentage of an extreme event at the selected location in Germany given blocking at a grid cell. The relevant blocking areas were subjectively identified based on the maxima in the spatial distribution of the two conditional frequencies.

The second step was a deepened analysis of the link between blocking in the identified areas and extreme events. Following criterion was determined: If more than 50% of the grid cells within the selected area were blocked, the day was counted as a blocking day. This definition and the daily information about the occurrence of extreme events enable to count the number of days with/without blocking/extreme event, and to populate a contingency table.

Based on the contingency table, we calculated the frequency of blocking days f_{block} and the frequency of extreme event days f_{ext}. Following the definitions in Table A1, the two marginal frequencies are calculated by

$$f_{block} = \frac{hits + false\ alarms}{n_{days}} = \frac{n_{blocking\ days}}{n_{days}}, \tag{2}$$

$$f_{ext} = \frac{hits + misses}{n_{days}} = \frac{n_{extreme\ event\ days}}{n_{days}}. \tag{3}$$

Furthermore, we calculated the frequency of blocking during an extreme event at a selected grid point $f_{block|ext}$, the frequency of an extreme event during blocking $f_{ext|block}$, and the frequency of an extreme event without blocking $f_{ext|no\ block}$. Following the definitions in Table A1, the three conditional frequencies are calculated by

$$f_{block|ext} = \frac{hits}{hits + misses} = \frac{hits}{n_{extreme\ event\ days}}, \tag{4}$$

$$f_{ext|block} = \frac{hits}{hits + false\ alarms} = \frac{hits}{n_{blocking\ days}}, \tag{5}$$

$$f_{ext|no\ block} = \frac{misses}{misses + correct\ rejections} = \frac{misses}{n_{no\ blocking\ days}}. \tag{6}$$

A further calculated quantity is the odds ratio, OR. The term *odds* describes the ratio between the probability that an event will happen and that it will not happen. The OR is the ratio of the odds of an event given a risk factor to the odds of the same

https://doi.org/10.5194/egusphere-2025-3670
Preprint. Discussion started: 19 September 2025

event without the risk factor (Bland, 2000; Stephenson, 2000). In the context of blocking and extreme events, the OR compares the odds of an extreme event with blocking with the odds of an extreme event without blocking as

$$OR = \frac{\frac{f_{ext|block}}{1 - f_{ext|block}}}{\frac{f_{ext|no\ block}}{1 - f_{ext|no\ block}}}, \tag{7}$$

which can be rewritten as

$$OR = \frac{hits \cdot correct\ rejections}{false\ alarms \cdot misses}. \tag{8}$$

An OR larger 1 indicates higher odds of an extreme event with blocking than without. An OR smaller or equal 1 indicates lower or equal odds of an extreme event with blocking than without. Significance of the ORs was tested at the 5% level with a two-sided Fisher's exact test by using the R function fisher.test from the stats package (R Core Team, 2024) (which applies the method by Bailey (1995)) (Ruxton and Neuhäuser, 2010, 2013).

Furthermore, contingency tables with the sum over all reanalyses respectively CMIP6 simulations, were calculated by adding the entries of the contingency tables of each reanalysis or simulation, here exemplarily for the hits:

$$hits_{tot} = \sum_{i=1}^{N} hits_i, \tag{9}$$

where N is the number of reanalyses respectively CMIP6 simulations. The other three entries in the contingency table according to the definitions in Table A1 were calculated analogously. Based on this contingency table, conditional frequencies, ORs and their significance were calculated for the average of the reanalyses respectively the CMIP6 simulations.

3 Results

This section presents the link between blocking and the introduced extreme events in present (1961-2010) and future (2051-2100).

3.1 Blocking and heatwaves

We present separately summer heatwaves (April to September) and winter heatwaves (October to March). Additionally, we discriminate between all heatwaves and strong heatwaves (HWMD>15).

3.1.1 Blocking and summer heatwaves

Figure 1 shows the frequency of blocking during heatwaves in Central Germany (at the marked point) and the frequency of heatwaves in Central Germany during blocking in ERA5 in the summer half-year. Blocking occurred at up to 45% of the heatwave days with a frequency maximum in the southern Baltic Sea. Heatwaves were most frequent during blocking in Central Europe (during up to 25% of the blocking days).

https://doi.org/10.5194/egusphere-2025-3670
Preprint. Discussion started: 19 September 2025

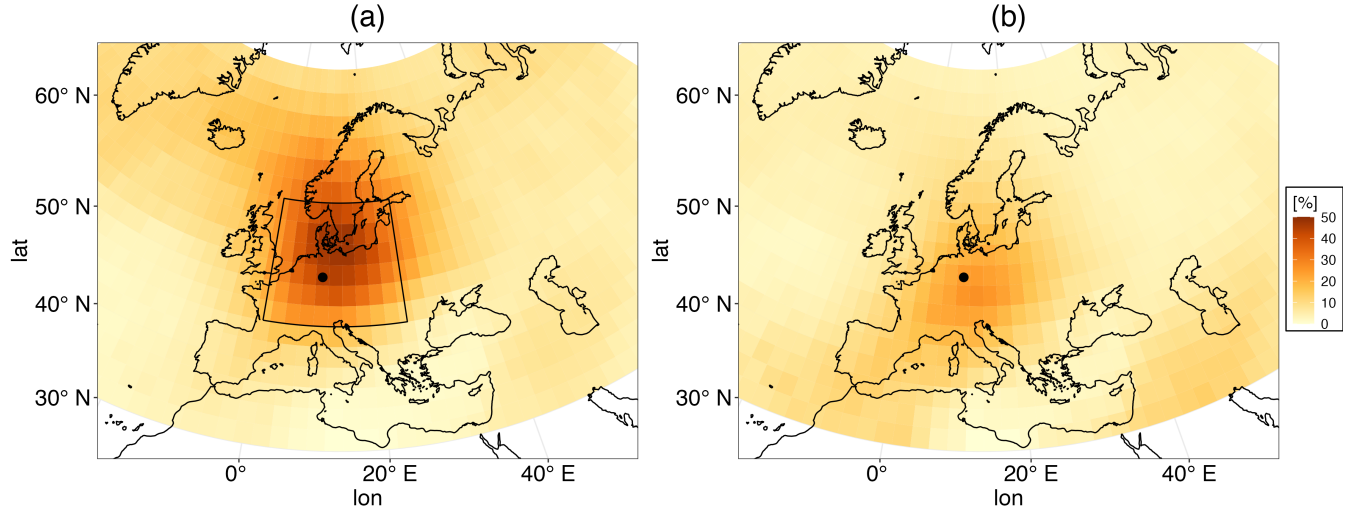

Figure 1. Frequency of blocking at a certain grid cell during summer heatwaves (April-September) at the marked point (51° N, 10° E; a); frequency of summer heatwaves at the marked point if there is blocking at a certain grid cell (b), both in ERA5 during the period 1961-2010. The black box in (a) denotes the area used to count blocking days.

Based on the spatial frequency distributions in Fig. 1, we identified an area from 0° to 25° E and from 45° N to 60° N as being relevant for heatwaves and calculated the marginal (Eq. 2-3) and conditional frequencies (Eq. 4-6) and ORs (Eq. 8) for the area averages. Averaged over the three investigated reanalyses, the frequency of heatwave days f_{HW} was 4.0% (4.7% in the mean of the historical CMIP6 simulations) and the frequency of blocking days f_{block} was 6.9% (6.0% in CMIP6). The frequency of blocking during heatwaves $f_{block|HW}$ was 40% in the mean of the reanalyses (see Table 1) with a good agreement between the three reanalyses (see Table S1). All historical CMIP6 simulations underestimated all reanalyses (see Table S1) with on average 33% (Table 1). The frequency of heatwaves during blocking $f_{HW|block}$ was approximately 23% in the mean of the reanalyses with a range of approximately 20 to 25%. On average, the simulations slightly overestimated $f_{HW|block}$ (26%). The frequency of heatwaves without blocking $f_{HW|no\ block}$ was 2.6% in the reanalyses and 3.4% in the CMIP6 simulations on average. The OR was 11 in the reanalyses and significant (9.9 in the CMIP6 simulations and significant).

In the mean of the reanalyses, the frequency of strong heatwave days with HWMD>15 f_{HW15} was 0.4% (0.8% in the mean of the CMIP6 simulations), and f_{block} did not change. During strong heatwaves, the frequency of blocking $f_{block|HW15}$ was approximately 68% in the mean of the reanalyses and highest in ERA-20C (see Table S2). All historical CMIP6 simulations underestimated all reanalyses (Table S2) with on average 41% (Table 1). The frequency of strong heatwaves during blocking $f_{HW15|block}$ reduced to 4.2% and the frequency of strong heatwaves without blocking $f_{HW15|no\ block}$ reduced to 0.1% in the average of the reanalyses. On average, the CMIP6 simulations overestimated both, $f_{HW15|block}$ (5.2%) and $f_{HW15|no\ block}$ (0.5%). The OR was 30 (with a wide range from approximately 20 to 40 in the individual reanalyses, significant in all reanaly-

https://doi.org/10.5194/egusphere-2025-3670
Preprint. Discussion started: 19 September 2025

Table 1. Conditional frequencies and odds ratios related to heatwaves (all or with HWMD>15, April-September) in Central Germany (51° N, 10° E) averaged over reanalyses and CMIP6 simulations during the period 1961-2010. Odds ratios in bold are significant at the 5% level.

	All HW		HWMD>15	
	Reanalyses	CMIP6 Simulations	Reanalyses	CMIP6 Simulations
$f_{block\|HW}$ [%]	39.7	32.8	68.4	41.4
$f_{HW\|block}$ [%]	22.9	25.6	4.2	5.2
$f_{HW\|no\ block}$ [%]	2.6	3.4	0.1	0.5
OR [-]	**11.2**	**9.9**	**30.4**	**11.5**

Table 2. As Table 1, but for the CMIP6 scenario SSP5-8.5 during the period 2051-2100, considering all heatwaves and heatwaves with HWMD>15.

	All HW	HWMD>15
$f_{block\|HW}$ [%]	27.3	34.7
$f_{HW\|block}$ [%]	80.4	61.2
$f_{HW\|no\ block}$ [%]	29.6	15.8
OR [-]	**9.8**	**8.4**

ses) and significant. All CMIP6 simulations underestimated the OR with on average 12, but the ORs of all CMIP6 simulations were significant.

For the future period (2051-2100), the models simulated on average an increase of f_{HW} to 36% and an increase of f_{block} to 12%. On average, $f_{block|HW}$ decreases to 27%, but $f_{block|HW}$ increases in two simulations (see Table S3). Concurrently, the projected $f_{HW|block}$ (80% on average) and $f_{HW|no\ block}$ (30% on average) increase. The ensemble range increased compared to simulations of the period 1961-2010 (see Table S3). The ensemble mean's OR is 9.8 and similar to the historical period, and significant. The OR increases in three simulations, especially in the UKESM1-0-LL (see Table S3).

On average, f_{HW15} increases to 21%. The frequency of blocking during strong heatwaves decreases to 35% in the ensemble mean (Table 2), but increases in two simulations (Table S4). Concurrently, $f_{HW15|block}$ (61%) and $f_{HW15|no\ block}$ (16%) increase in the mean. The ensemble's mean OR decreases to 8.4, but is still significant. The OR increases in the CESM2 and the UKESM1-0-LL and shows, as the three conditional frequencies, a wide range in the ensemble (Table S4).

3.1.2 Blocking and winter heatwaves

Analogue to Fig. 1, but for the winter half-year, Fig. 2 shows the frequency of blocking during heatwaves in Central Germany and the frequency of heatwaves in Central Germany during blocking. Blocking occurred most frequently over the Alps and Northern Italy. Approximately 25 to 30% of the heatwave days had blocking in this area. Heatwaves were most frequent if

https://doi.org/10.5194/egusphere-2025-3670
Preprint. Discussion started: 19 September 2025

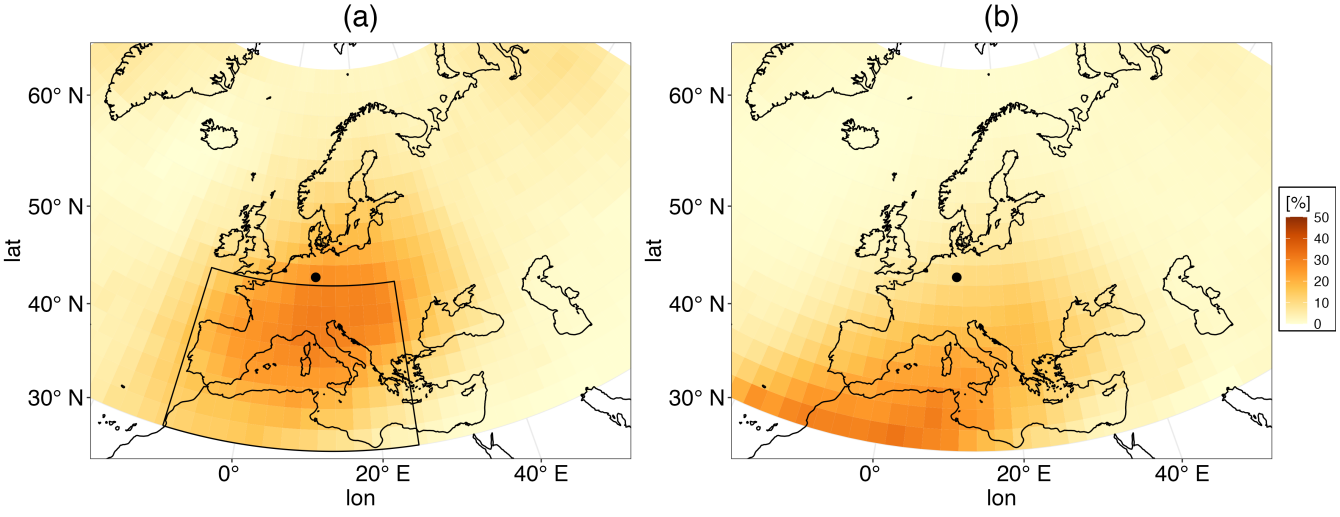

Figure 2. As Fig. 1, but for winter heatwaves (October-March).

blocking was over the Western Mediterranean and North Africa. In approximately 25 to 30% of the blocking days there, a heatwave occurred in Central Germany.

Based on the spatial frequency distributions in Fig. 2, we selected an area from 10° W to 25° E and from 30° N to 50° N (see Fig. 2a) and calculated the marginal and conditional frequencies and the ORs for the area averages. Note that this region is more in the south than the selected area for summer heatwaves. Averaged over the three reanalyses, f_{HW} was 3.7% (3.8% in the mean of the CMIP6 simulations) and f_{block} was 2.9% (2.7% in CMIP6). In the mean of the three reanalyses, $f_{block|HW}$ was 19% (only approximately 50% of the summer frequency, Table 3). On average, the CMIP6 simulations underestimated $f_{block|HW}$ (13%). $f_{HW|block}$ was 24% in the reanalyses (Table 3) and underestimated by the CMIP6 simulations (18%). Both conditional frequencies show a wide range between the three reanalyses (with the highest values in ERA5) and in the CMIP6 ensemble (see Table S5). Similarly to the summer half-year, $f_{HW|no\ block}$ was low (3.1% in the average of the reanalyses). On average, $f_{HW|no\ block}$ was slightly higher in the CMIP6 simulations (3.4%). The OR was 9.8 (similar to the summer OR) and significant in the reanalyses, but with a large spread (see Table S5). The CMIP6 simulations underestimated the OR (6.4, but mean OR of CMIP6 simulations was significant).

In the mean of the reanalyses, f_{HW15} was 0.4% (0.4% in CMIP6). During strong heatwaves, the frequency of blocking $f_{block|HW15}$ was 15% in the mean of the reanalyses (Table 3) and highest in ERA-20C (Table S6). On average, $f_{block|HW15}$ agreed between the historical CMIP6 simulations and the reanalyses, but $f_{block|HW15}$ has a wide range in the CMIP6 ensemble (Table S6). In the mean of the reanalyses, $f_{HW15|block}$ reduced to 2.3%. The CMIP6 agreed with the reanalyses on average (2.4%), but the CMIP6 ensemble shows a wide range (Table S6). In the mean of both, reanalyses and CMIP6 simulations, $f_{HW15|no\ block}$ reduced to 0.4%. The OR reduced to 6.1 in the reanalyses (only approximately 20% of the summer OR) and was again 6.4 in the CMIP6 simulations. The OR was significant in both, reanalyses and CMIP6 simulations. However, the

https://doi.org/10.5194/egusphere-2025-3670
Preprint. Discussion started: 19 September 2025

Table 3. As Table 1, but for winter heatwaves (October-March).

	All HW		HWMD>15	
	Reanalyses	CMIP6 Simulations	Reanalyses	CMIP6 Simulations
$f_{block\|HW}$ [%]	18.8	13.2	15.1	15.0
$f_{HW\|block}$ [%]	24.2	18.2	2.3	2.4
$f_{HW\|no\ block}$ [%]	3.1	3.4	0.4	0.4
OR [-]	**9.8**	**6.4**	**6.1**	**6.4**

Table 4. As Table 3, but for the CMIP6 scenario SSP5-8.5 during the period 2051-2100, considering all heatwaves and heatwaves with HWMD>15.

	All HW	HWMD>15
$f_{block\|HW}$ [%]	10.2	13.5
$f_{HW\|block}$ [%]	63.5	42.5
$f_{HW\|no\ block}$ [%]	25.4	12.4
OR [-]	**5.1**	**5.2**

CMIP6 ensemble shows a wide range and the NorESM2-MM did not simulate any strong heatwave related to blocking in the winter half-year (Table S6).

For the future period (2051-2100), the models simulated on average an increase of f_{HW} to 27% and an increase of f_{block} to 4.3%. In the ensemble mean, $f_{block|HW}$ reduces to 10% (see Table 4). The spread of $f_{block|HW}$ in the ensemble is small (Table S7). In the ensemble mean, $f_{HW|block}$ increases to 64% and $f_{HW|no\ block}$ increases to 25%. In the ensemble, the spread of $f_{HW|block}$ and $f_{HW|no\ block}$ increases compared to the historical period (Table S7). The ensemble's mean OR reduces to 5.1, but is still significant.

The frequency of strong heatwaves increases to 14% and the frequency of blocking during strong heatwaves reduces to 14% in the ensemble mean (see Table 4), but $f_{block|HW15}$ increases in three simulations (Table S8). The frequency of strong heatwaves during blocking increases on average to 43%, and the frequency of strong heatwaves without blocking increases on average to 12%. The ensemble's mean OR is 5.2 and significant, but lower than in the historical period.

3.2 Blocking and heavy precipitation

Figure 3 shows the frequencies of blocking during heavy precipitation and of heavy precipitation during blocking in Western and Eastern Germany respectively in the annual mean. During heavy precipitation in Western Germany, blocking was most frequent over Scandinavia with a frequency of 10-15% (Fig. 3a). Heavy precipitation in Western Germany was most frequent (up to 3%) if the block was over the Atlantic close to the Azores (Fig. 3b). The frequency of heavy precipitation in Western

https://doi.org/10.5194/egusphere-2025-3670
Preprint. Discussion started: 19 September 2025

Germany was below 1% if the block was in Northern or Eastern Europe. The low frequencies of heavy precipitation during blocking were related to the definition of heavy precipitation: since the threshold is the 99th percentile, only approximately 1% of all days were heavy precipitation days.

During heavy precipitation in Eastern Germany, the frequency of blocking was 20-25% over Scandinavia and approximately 15% over Eastern Europe (Fig. 3c). The frequency of heavy precipitation in Eastern Germany during blocking in Eastern or Northern Europe was approximately 2% (Fig. 3d).

Based on the spatial frequency distributions in Fig. 3, we selected two areas, one in Scandinavia (from 0° to 40° E and from 60° N to 75° N) and one in Eastern Europe (from 30° E to 60° E and from 40° N to 60° N) and calculated the marginal and conditional frequencies and the ORs for the area averages. As for heatwaves, the investigation was done separately for the summer (April-September) and winter half-year (October-March) because of different synoptic patterns in winter and summer (Hofstätter et al., 2018). In the summer half-year, the frequency of heavy precipitation days in Western Germany $f_{Pr,W}$ was 0.7% in the mean of the reanalyses (1.1% in the mean of the CMIP6 simulations), and the frequencies of blocking days over Scandinavia $f_{block,Scan}$ and over Eastern Europe $f_{block,EE}$ were 11% respectively 5.0% (9.6% respectively 4.1% in CMIP6). The frequency of blocking over Scandinavia during heavy precipitation in Western Germany $f_{block,Scan|Pr,W}$ was 17% and the frequency of blocking over Eastern Europe during heavy precipitation in Western Germany $f_{block,EE|Pr,W}$ was 9.6% in the mean of the reanalyses (Table 5). All historical CMIP6 simulations underestimated the reanalyses with on average 11% ($f_{block,Scan|Pr,W}$) and 4.5% ($f_{block,EE|Pr,W}$) (Table S9). In the mean of the reanalyses, the frequency of heavy precipitation in Western Germany during blocking over Scandinavia $f_{Pr,W|block,Scan}$ and the frequency of heavy precipitation in Western Germany during blocking over Eastern Europe $f_{Pr,W|block,EE}$ were 1.1% respectively 1.4%. On average, the CMIP6 simulations slightly overestimated $f_{Pr,W|block,Scan}$ (1.3%) and slightly underestimated $f_{Pr,W|block,EE}$ (1.2%) (Table 5). In the mean of the reanalyses, the frequencies of heavy precipitation in Western Germany without blocking over Scandinavia $f_{Pr,W|no\ block,Scan}$ and without blocking over Eastern Europe $f_{Pr,W|no\ block,EE}$ were 0.7%. On average, the CMIP6 simulations overestimated $f_{Pr,W|no\ block,Scan}$ and $f_{Pr,W|no\ block,EE}$ (1.1% each). The ORs were 1.7 (Scandinavian blocking) and 2.1 (Eastern European blocking) in the reanalyses, and both significant. In the mean of the CMIP6 simulations, the ORs were 1.1 (Scandinavia) and 1.2 (Eastern Europe), and both not significant and with ORs<1 in the ensemble (Table S9).

The frequency of heavy precipitation days in Eastern Germany $f_{Pr,E}$ was 1.5% in the mean of the reanalyses (1.4% in CMIP6), and $f_{block,Scan}$ and $f_{block,EE}$ were identical to the previous paragraph. Averaged over the three investigated reanalyses, the frequency of blocking over Scandinavia during heavy precipitation in Eastern Germany $f_{block,Scan|Pr,E}$ was 18% and the frequency of blocking over Eastern Europe during heavy precipitation in Eastern Germany $f_{block,Scan|Pr,E}$ was 9.7%. On average, the historical CMIP6 simulations underestimated $f_{block,Scan|Pr,E}$ (13%) and $f_{block,EE|Pr,E}$ (6.6%). The frequency of heavy precipitation in Eastern Germany during blocking over Scandinavia $f_{Pr,E|block,Scan}$ was 2.4% and the frequency of heavy precipitation in Eastern Germany during blocking over Eastern Europe $f_{Pr,E|block,EE}$ was 2.9%, both in the mean of the reanalyses. On average, the CMIP6 simulations underestimated $f_{Pr,E|block,Scan}$ (1.4%) and $f_{Pr,E|block,EE}$ (2.3%). The frequencies of heavy precipitation in Eastern Germany without blocking over Scandinavia $f_{Pr,E|no\ block,Scan}$ and Eastern Europe $f_{Pr,E|no\ block,EE}$ were both 1.4% in the mean of the reanalyses. The CMIP6 simulations agreed on average with the

https://doi.org/10.5194/egusphere-2025-3670
Preprint. Discussion started: 19 September 2025

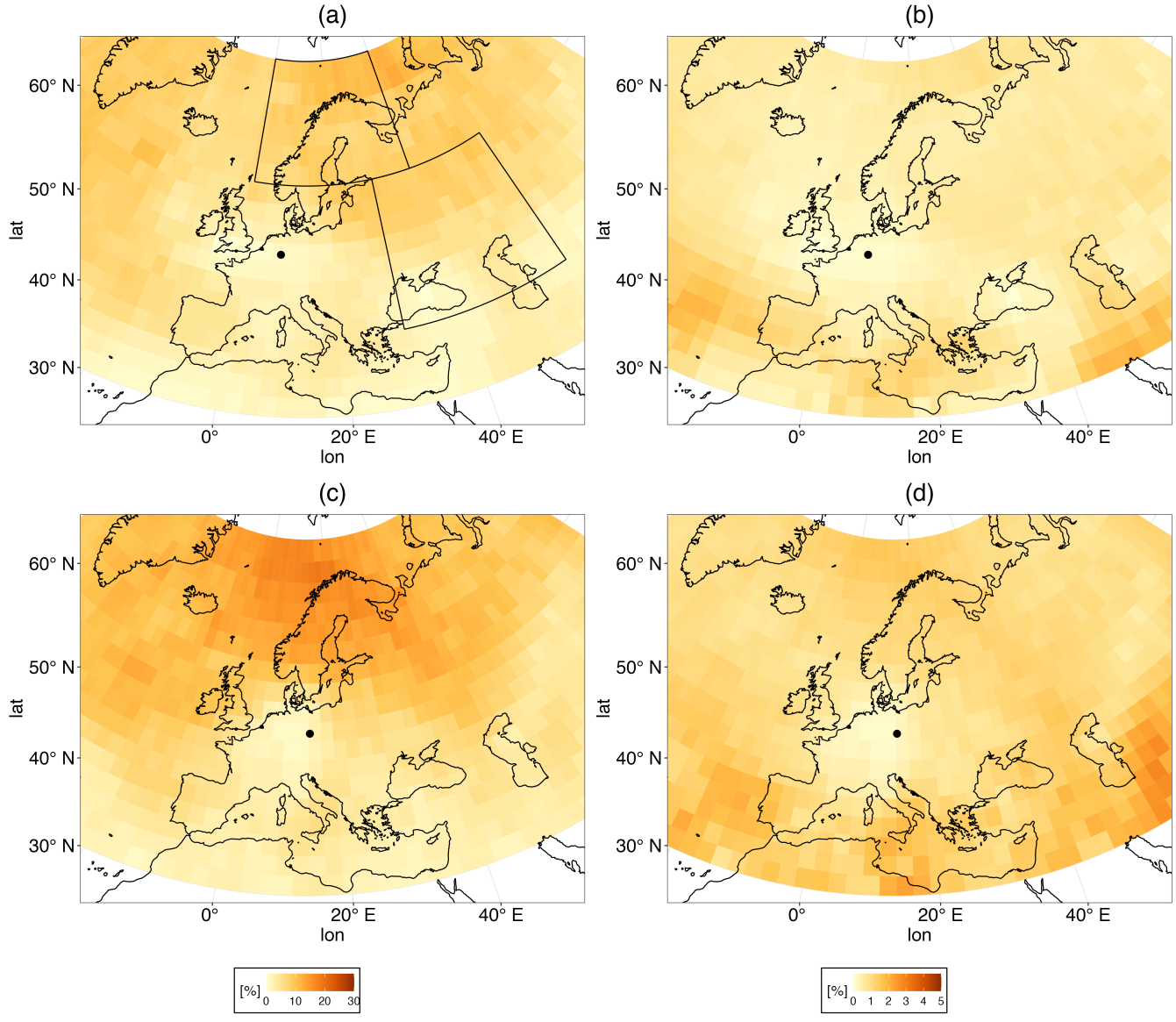

Figure 3. Frequencies of blocking at a certain grid cell during heavy precipitation at the marked point (a,c); frequencies of heavy precipitation at the marked point if there is blocking at a certain grid cell (b,d). (a,b): Heavy precipitation in Western Germany (51° N, 8° E); (c,d): Heavy precipitation in Eastern Germany. (51° N, 14° E). All subplots refer to ERA5 during the period 1961-2010. The boxes in (a) denote the areas used to count blocking days. Note the different scales between the two conditional frequencies.

reanalyses (Table 5). The ORs were 1.7 (Scandinavian blocking) and 2.1 (Eastern European blocking) in the reanalyses, and both significant. The CMIP6 ensemble's mean ORs were 1.4 (Scandinavia) and 1.7 (Eastern Europe) and significant.

https://doi.org/10.5194/egusphere-2025-3670
Preprint. Discussion started: 19 September 2025

Table 5. Conditional frequencies related to heavy precipitation (April-September) in Western (51° N, 8° E, top) and Eastern Germany (51° N, 14° E, bottom) averaged over reanalyses and CMIP6 simulations during the period 1961-2010. The abbreviation "EE" denotes blocking over Eastern Europe and "Scan" blocking over Scandinavia. The abbreviation "Pr" in the index of the conditional frequencies denotes heavy precipitation. Odds ratios in bold are significant at the 5% level.

	Reanalyses		CMIP6 Simulations	
	Western Germany			
	EE	Scan	EE	Scan
$f_{block\|Pr}$ [%]	9.6	17.2	4.5	11.3
$f_{Pr\|block}$ [%]	1.4	1.1	1.2	1.3
$f_{Pr\|no\ block}$ [%]	0.7	0.7	1.1	1.1
OR [-]	**2.1**	**1.7**	1.1	1.2
	Eastern Germany			
	EE	Scan	EE	Scan
$f_{block\|Pr}$ [%]	9.7	17.8	6.6	13.0
$f_{Pr\|block}$ [%]	2.9	2.4	2.3	1.4
$f_{Pr\|no\ block}$ [%]	1.4	1.4	1.4	1.4
OR [-]	**2.1**	**1.7**	**1.7**	**1.4**

In the winter half-year (October-March), $f_{Pr,W}$ was 0.9% in the mean of the reanalyses (0.8% in CMIP6), and $f_{block,Scan}$ and $f_{block,EE}$ were 11.3% respectively 4.7% (11.1% respectively 4.6% in CMIP6). In the average of the three reanalyses, $f_{block,Scan|Pr,W}$ and $f_{block,EE|Pr,W}$ reduced to less than 1% (Table 6). The historical CMIP6 simulations overestimated on average both $f_{block|Pr,W}$ (Table 6). In the mean of the reanalyses, $f_{Pr,W|block,Scan}$ reduced to 0.03% and $f_{Pr,W|block,EE}$ reduced to 0.2%. The CMIP6 simulations overestimated on average both $f_{Pr,W|block}$. In the mean of the reanalyses, $f_{Pr,W|no\ block,Scan}$ and $f_{Pr,W|no\ block,EE}$ increased to 1.0%, and the CMIP6 simulations slightly underestimated the frequency of heavy precipitation without blocking. The ORs were 0.03 (Scandinavian blocking) and 0.2 (Eastern European blocking) in the reanalyses and significant. The ORs in the CMIP6 simulations were 0.25 (Scandinavia) and 0.4 (Eastern Europe), and both ORs were significant.

In the mean of the three reanalyses, $f_{Pr,E}$ was 0.5% (0.5% in CMIP6), and $f_{block,Scan}$ and $f_{block,EE}$ were identical to the previous paragraph. In the mean of the reanalyses, $f_{block,Scan|Pr,E}$ and $f_{block,EE|Pr,E}$ were 4-5% (Table 6). On average, the historical CMIP6 simulations overestimated $f_{block,Scan|Pr,E}$ (5.6%) and $f_{block,EE|Pr,E}$ (7.1%). In the mean of the reanalyses, $f_{Pr,E|block,Scan}$ reduced to 0.2% and $f_{Pr,W|block,EE}$ reduced to 0.4%. In the CMIP6 mean, $f_{Pr,E|block,EE}$ was overestimated (0.7%), but $f_{Pr,E|block,Scan}$ agreed with the reanalyses. In the mean of the reanalyses, $f_{Pr,E|no\ block,Scan}$ and $f_{Pr,E|no\ block,EE}$ were 0.5% and the CMIP6 simulations agreed on average with the reanalyses (Table 6). The ORs were 0.4

https://doi.org/10.5194/egusphere-2025-3670
Preprint. Discussion started: 19 September 2025

Table 6. As Table 5, but for the winter half-year (October-March).

	Reanalyses		CMIP6 Simulations	
	Western Germany			
	EE	Scan	EE	Scan
$f_{block\|Pr}$ [%]	0.8	0.4	1.9	3.1
$f_{Pr\|block}$ [%]	0.2	0.03	0.3	0.2
$f_{Pr\|no\ block}$ [%]	1.0	1.0	0.8	0.9
OR [-]	**0.2**	**0.03**	**0.4**	**0.25**
	Eastern Germany			
	EE	Scan	EE	Scan
$f_{block\|Pr}$ [%]	4.0	4.8	7.1	5.6
$f_{Pr\|block}$ [%]	0.4	0.2	0.7	0.2
$f_{Pr\|no\ block}$ [%]	0.5	0.5	0.4	0.5
OR [-]	0.9	**0.4**	1.6	**0.5**

(Scandinavian blocking) and 0.9 (Eastern European blocking) in the reanalyses and only the OR of Scandinavian blocking was significant. The ORs in the CMIP6 mean were 0.5 (Scandinavia) and 1.6 (Eastern Europe) and consequently overestimated, but only the OR of Scandinavian blocking was significant. The ORs of Eastern European blocking have a wide range from 0.0 to 3.7 in the ensemble (Table S10).

In the summer half-year of the future period, $f_{Pr,W}$ increases to 1.4% in the mean of the CMIP6 SSP5-8.5 scenario simulations, and $f_{block,Scan}$ and $f_{block,EE}$ increase to 15% respectively 11%. In the ensemble mean, $f_{block,Scan|Pr,W}$ and $f_{block,EE|Pr,W}$ increase to 18% respectively 12% (Table 7) with the most pronounced increases in the CESM2 and NorESM2-MM (see Table S11). In the ensemble mean, $f_{Pr,W|block,Scan}$ increases to 1.7% and $f_{Pr,W|block,EE}$ increases to 1.5%. Furthermore, $f_{Pr,W|no\ block,Scan}$ and $f_{Pr,W|no\ block,EE}$ increase to 1.4% (both blocking regions). The projected OR of Scandinavian blocking is 1.2 (significant) and the OR of Eastern European blocking is 1.1 (not significant) (Table 7).

In the CMIP6 ensemble mean, $f_{Pr,E}$ increases to 1.8%, and $f_{block,Scan}$ and $f_{block,EE}$ are identical to the previous paragraph. Furthermore, $f_{block,Scan|Pr,E}$ and $f_{block,EE|Pr,E}$ increase to 18% respectively 11% (Table 7). Again, the increase is most pronounced in the CESM2 and NorESM2-MM (Table S11). In the CMIP6 ensemble mean, $f_{Pr,E|block,Scan}$ increases to 2.1% and $f_{Pr,E|block,EE}$ reduces to 1.7%. $f_{Pr,E|no\ block,Scan}$ and $f_{Pr,E|no\ block,EE}$ increase to 1.7% respectively 1.8%. The ORs reduce to 1.2 (significant, Scandinavian blocking) and 0.9 (not significant, Eastern European blocking).

In the winter half-year of the future period, $f_{Pr,W}$ increases on average to 1.5 %, and $f_{block,Scan}$ and $f_{block,EE}$ increase to 11.8% respectively 6.9%. $f_{block,Scan|Pr,W}$ and $f_{block,EE|Pr,W}$ increase on average to approximately 3% (Table 7). In the ensemble mean, $f_{Pr,W|block,Scan}$ increases to 0.4% and $f_{Pr,W|block,EE}$ increases to 0.7%. Furthermore, $f_{Pr,W|no\ block,Scan}$

https://doi.org/10.5194/egusphere-2025-3670
Preprint. Discussion started: 19 September 2025

Table 7. Conditional frequencies related to heavy precipitation in summer (April-September) and winter (October-March) in Western (51° N, 8° E) and Eastern Germany (51° N, 14° E) averaged over CMIP6 simulations during the period 2051-2100 assuming the CMIP6 scenario SSP5-8.5. The abbreviation "EE" denotes blocking over Eastern Europe and "Scan" blocking over Scandinavia. The abbreviation "Pr" in the index of the conditional frequencies denotes heavy precipitation. Odds ratios in bold are significant at the 5% level.

	Summer		Winter	
	Western Germany			
	EE	Scan	EE	Scan
$f_{block\|Pr}$ [%]	11.9	17.6	3.3	3.2
$f_{Pr\|block}$ [%]	1.5	1.7	0.7	0.4
$f_{Pr\|no\ block}$ [%]	1.4	1.4	1.6	1.6
OR [-]	1.1	**1.2**	**0.5**	**0.2**
	Eastern Germany			
	EE	Scan	EE	Scan
$f_{block\|Pr}$ [%]	10.7	17.6	8.4	9.4
$f_{Pr\|block}$ [%]	1.7	2.1	1.0	0.6
$f_{Pr\|no\ block}$ [%]	1.8	1.7	0.8	0.8
OR [-]	0.9	**1.2**	1.2	0.8

and $f_{Pr,W|no\ block,EE}$ increase to 1.6%. The ORs are 0.2 (Scandinavian blocking) and 0.5 (Eastern European blocking) and both significant.

In the ensemble mean, $f_{Pr,E}$ increases to 0.8% ($f_{block,Scan}$ and $f_{block,EE}$ are identical to the previous paragraph) whereas $f_{block,Scan|Pr,E}$ and $f_{block,EE|Pr,E}$ increase to 8-9% (Table 7). $f_{Pr,E|block,Scan}$ increases to 0.6% and $f_{Pr,E|block,EE}$ increases to 1.0%. Furthermore, $f_{Pr,E|no\ block,Scan}$ and $f_{Pr,E|no\ block,EE}$ increase to 0.8%.The ORs are 0.8 (Scandinavian blocking) and 1.2 (Eastern European blocking) and are not significant. The Eastern European ORs have a wide range from 0.4 to 2.1 in the ensemble (see Table S12).

3.3 Blocking and calms

Figure 4 shows the frequency of blocking during calms and the frequency of calms during blocking. During calms in Central Germany, blocking was most frequent over Northern Central Europe and the North Sea with 20-25% of the calm days. Calms were most frequent (at approximately 10% of the days) if the block was over Central Europe.

Based on the spatial frequency distributions in Fig. 4, we selected an area from 10° W to 25° E and from 50° N to 65° N (see Fig. 4a) and calculated the conditional and marginal frequencies and the ORs for the area averages. The period of interest was the winter half-year (October-March), since periods of low solar and wind energy production occurred only during this

https://doi.org/10.5194/egusphere-2025-3670
Preprint. Discussion started: 19 September 2025

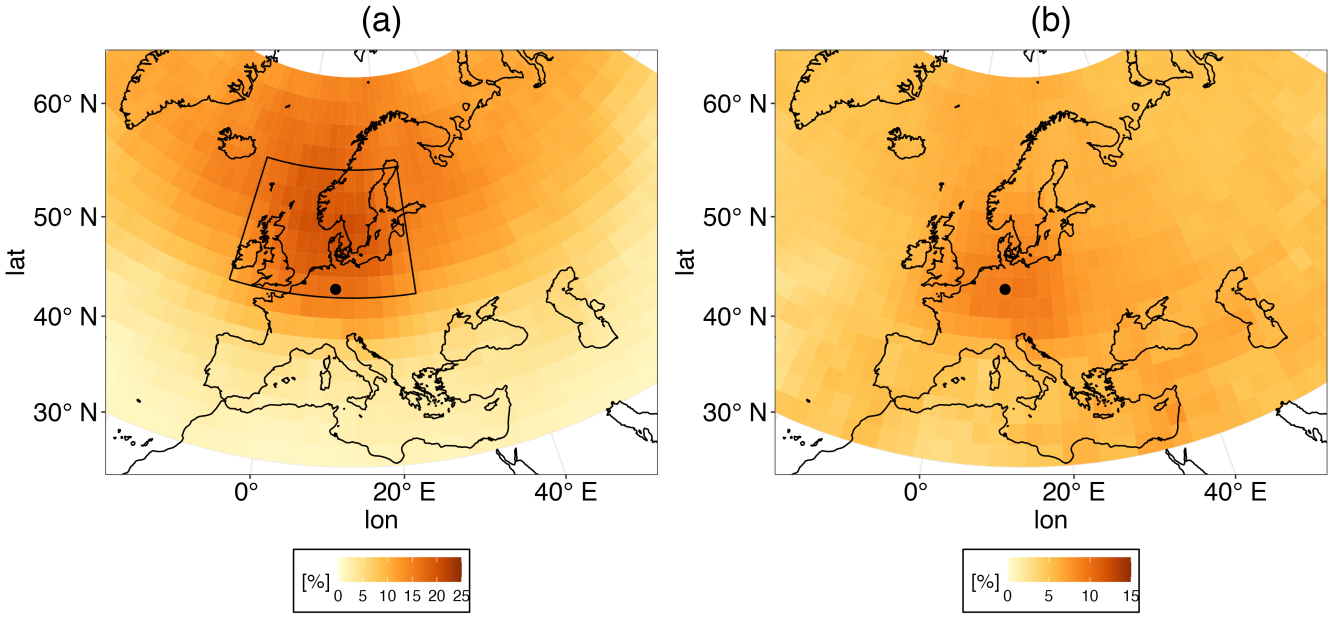

Figure 4. Frequency of blocking at a certain grid cell during calms at the marked point (51° N, 10° E; a); frequency of calms at the marked point if there is blocking at a certain grid cell (b). Both subplots refer to calms in ERA5 during the period 1961-2010. The box in (a) denotes the area used to count blocking days. Note the different scales between the two conditional frequencies.

time of the year (Drücke et al., 2021). During the winter half-year, the frequency of calm days f_{calm} was 4.1% in the mean of the three reanalyses (2.9% in the mean of the CMIP6 simulations) and the frequency of blocking days f_{block} was 10% (10% in CMIP6). The frequency of blocking during calms $f_{block|calm}$ was 21% averaged over the reanalyses (Table 8). On average, the CMIP6 simulations overestimated $f_{block|calm}$ (26%), including a wide range (Table S14). The frequency of calms during blocking $f_{calm|block}$ was 8.2% in the reanalyses. The CMIP6 simulations slightly underestimated $f_{calm|block}$ with on average 7.4%, showing a wide range. The frequency of calms without blocking $f_{calm|no\ block}$ was 3.7% in the reanalyses and 2.4% in the CMIP6 simulations. The OR was 2.4 in the reanalyses and 3.3 in the CMIP6 simulations. Both ORs were significant. The link between blocking and calms was strongest in ERA5 and weakest in ERA-20C (Table S14).

During the summer half-year (April-September), the OR was 1.1 and not significant in the mean of the reanalyses with good agreement between the reanalyses (Table S13). The CMIP6 simulations overestimated the OR with on average 1.6 and the OR was significant (Table 8).

In the mean of the SSP5-8.5 scenario simulations of the future winter half-year, f_{calm} and f_{block} increase to 3.8% respectively 11%. $f_{block|calm}$ increases to on average 30% (Table 9) with a wide range (see Table S16). In the mean of the CMIP6 simulations, $f_{calm|block}$ increases to 10% and $f_{calm|no\ block}$ to 3.0% (Table 9). The OR is 3.6 and significant.

During the summer half-year, the OR decreases to on average 1.3, but the OR is significant. The conditional frequencies have a wide range in the ensemble (Table S15).

https://doi.org/10.5194/egusphere-2025-3670
Preprint. Discussion started: 19 September 2025

Table 8. Conditional frequencies related to calms in Central Germany (51° N, 10° E) averaged over reanalyses and CMIP6 simulations during the period 1961-2010, considering the summer (April-September) and the winter half-year (October-March). Odds ratios in bold are significant at the 5% level.

	Summer		Winter	
	Reanalyses	CMIP6 Simulations	Reanalyses	CMIP6 Simulations
$f_{block\|calm}$ [%]	10.4	11.8	20.6	26.2
$f_{calm\|block}$ [%]	6.6	10.1	8.2	7.4
$f_{calm\|no\ block}$ [%]	5.9	6.5	3.7	2.4
OR [-]	1.1	**1.6**	**2.4**	**3.3**

Table 9. Conditional frequencies related to calms in Central Germany (51° N, 10° E) averaged over CMIP6 simulations during the period 2051-2100 assuming the CMIP6 scenario SSP5-8.5, considering the summer (April-September) and the winter half-year (October-March). Odds ratios in bold are significant at the 5% level.

	Summer	Winter
$f_{block\|calm}$ [%]	16.6	30.2
$f_{calm\|block}$ [%]	10.1	10.0
$f_{calm\|no\ block}$ [%]	7.7	3.0
OR [-]	**1.3**	**3.6**

4 Discussion

This study figured out the spatial distribution of blocking linked to extreme events and quantified the occurrence of the extreme events with and without blocking. After that, it compared the findings of the reanalyses to CMIP6 simulations and investigated future projections.

Figure 5 summarises the ORs in reanalyses and climate simulations. Heatwaves were the extreme events of the three analysed types (heatwave, heavy precipitation and calm events) with the highest ORs. In the summer half-year, the location of the block over Central Europe suggests that solar insolation and subsidence are the main drivers of heatwaves which supports previous research (Pfahl and Wernli, 2012; Pfahl, 2014; Zschenderlein et al., 2019; Kautz et al., 2022). Advection of warm air plays only a secondary role (Zschenderlein et al., 2019). Strong heatwaves (HWMD>15) had a strong link to blocking: their OR was higher than the OR of all heatwaves (see Table 1 and Fig. 5). Blocking forces soil desiccation and strong boundary layer growth in the wake of entrainment processes which were identified as key contributors to the extreme heatwaves of 2003 and 2010 in Europe (Miralles et al., 2014).

In the winter half-year, heatwaves were also linked to blocking, but in a different way. The blocks were located over the Alps and Southern Europe. In this case, Germany was on the northern flank of the block in a (south)western flow. This results

https://doi.org/10.5194/egusphere-2025-3670
Preprint. Discussion started: 19 September 2025

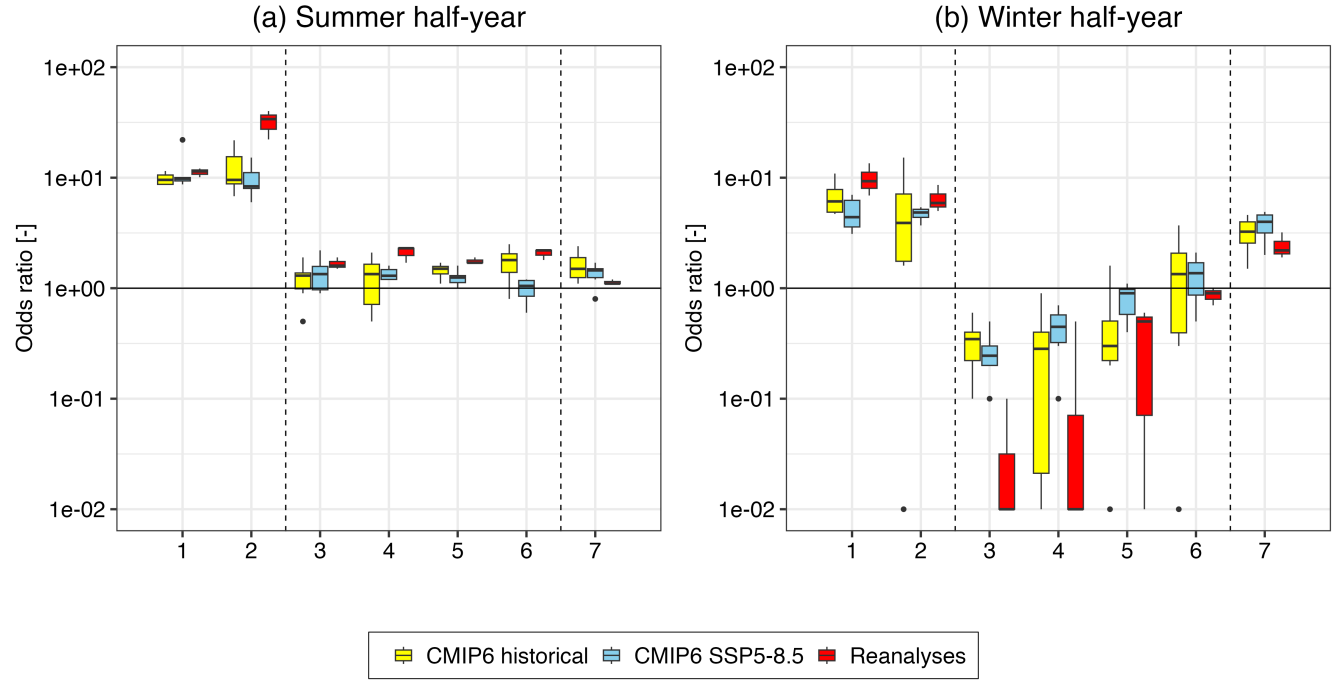

Figure 5. Odds ratios of the different extreme event types in reanalyses and CMIP6 climate simulations (historical and future) in summer (a) and winter half-year (b). The numbers along the x axis denote following extreme events: 1: heatwaves; 2: heatwaves with HWMD>15; 3: Scandinavian blocking and heavy precipitation in Western Germany; 4: Eastern European blocking and heavy precipitation in Western Germany; 5: Scandinavian blocking and heavy precipitation in Eastern Germany; 6: Eastern European blocking and heavy precipitation in Eastern Germany; 7: calms. The horizontal line denotes an odds ratio of 1. The vertical lines separate the three types of extreme events (heatwaves, heavy precipitation and calm events). Note that odds ratios equal to 0 were set to 0.01 to avoid values equal to minus infinity in the logarithmic scale.

in advection of warm air from the Atlantic (Holmberg et al., 2023; Tuel and Martius, 2024). Blocking was less frequent during winter heatwaves than during summer heatwaves and the OR was slightly lower than in summer. This indicates a weaker link between blocking and winter heatwaves than summer heatwaves. Heatwaves with HWMD>15 had a weakened link to blocking: their OR was lower than the OR of all heatwaves (see Table 3 and Fig. 5). This is a fundamental difference to summer heatwaves and emphasises different mechanisms between summer and winter heatwaves. In winter, positive temperature anomalies in Central and Northern Europe were related to positive anomalies of eddy kinetic energy (i.e. high storm track activity) whereas positive temperature anomalies in summer were related to negative anomalies of eddy kinetic energy (i.e. low storm track activity and more blocking) (Lehmann and Coumou, 2015).

Overall, the CMIP6 simulations could simulate the link between blocking and heatwaves in the summer half-year which confirms Schaller et al. (2018). Heatwaves are large-scale phenomena that are resolved by climate models with low resolution.

https://doi.org/10.5194/egusphere-2025-3670
Preprint. Discussion started: 19 September 2025

However, the climate simulations underestimated the link between blocking and strong heatwaves (expressed by the OR) as shown in Table 1. One reason might be the underestimation of the persistence of the blocks: the lifetime of the blocks was underestimated by the simulations (Lohmann et al., 2024). Furthermore, the ORs of strong heatwaves have a wide range in the historical simulations (Fig.5).

The CMIP6 simulations underestimated the link between blocking and winter heatwaves. One potential reason is the underestimation of winter blocking over Europe in the climate simulations: if less blocking is simulated, $f_{block|HW}$ tends to be reduced. Furthermore, a too strong jetstream (Davini and D'Andrea, 2020) and a bias of storm tracks in CMIP6 (Priestley et al., 2020) might result in an increased fraction of cyclonic weather patterns related to heatwaves compared to the reanalyses. In this case, strong cyclones advect warm air from the Atlantic towards Central Europe without the occurrence of blocking. Interestingly, the CMIP6 simulations slightly overestimated the link between blocking and strong winter heatwaves, whereas the simulations underestimated the link between blocking and strong summer heatwaves. Again, the OR had a wide range in the ensemble (Fig.5).

For the future, the climate models simulated less blocking during heatwaves. This decrease is caused by the projected increase in heatwave days which is large compared to changes in blocking days. Thus, the relative fraction of blocking decreases. The ensemble mean's OR is similar to the historical period (see Table 1 and 2), but the OR of the UKESM1-0-LL is 22 and a strong outlier. Furthermore, this model projected a more pronounced increase in heatwave days (summer and winter) than the other models. The UKESM1-0-LL has a high climate sensitivity (Andrews et al., 2019; Dong et al., 2020), which could explain the pronounced increase in heatwave days. The other five simulations show on average a slightly decreased OR. The on average reduced OR in the other simulations is the result of changes in thermodynamics like increased mean temperature (Schaller et al., 2018) or reduced soil moisture (Suarez-Gutierrez et al., 2020). If the reference period for heatwave calculation was adapted to the future (e.g. 2070-2099), the link between blocking and heatwaves did not change (Schaller et al., 2018).

The comparison between $f_{Pr,W}$ and $f_{Pr,E}$ between the summer and the winter half-year shows that days with heavy precipitation are more frequent in Eastern than in Western Germany in the summer half-year and vice versa in the winter half-year which agrees with Lenggenhager and Martius (2019). Furthermore, the seasonal cycle of heavy precipitation days was more pronounced in Eastern Germany. The occurrence of heavy precipitation in Germany in the summer half-year was weakly linked to blocking over Eastern Europe and Scandinavia. This synoptic pattern slows down the eastward propagation of troughs or can cause the formation of cut-off lows over Central or Southern Europe which move only slowly resulting in high precipitation amounts (Kautz et al., 2022). However, the OR was approximately only 2 and therefore, the link between blocking and heavy precipitation was much weaker than the link to heatwaves, but still significant. Eastern European blocking had a slightly higher OR than Scandinavian blocking. Thus, blocking over Eastern Europe is more often linked to heavy precipitation than blocking over Scandinavia. The ORs of heavy precipitation in Western and Eastern Germany agree. This is surprising because the results of Hofstätter et al. (2018) suggest higher ORs in Eastern than in Western Germany. However, days with heavy precipitation are less frequent in Western than in Eastern Germany during the summer half-year. Averaged over the year, the OR of heavy precipitation is higher in Eastern than in Western Germany (not shown) which confirms Hofstätter et al. (2018). In the winter half-year, blocking over Northern and Eastern Europe reduces the odds of heavy precipitation which confirms the results by

https://doi.org/10.5194/egusphere-2025-3670
Preprint. Discussion started: 19 September 2025

Yao and De-Hai (2014). Heavy precipitation in winter is typically linked to cyclones which propagate eastward and advect moist air from the Atlantic to the continent (Hofstätter et al., 2018). In summer, blocking over Eastern Europe advects warm and moist air masses to Central Europe (Mohr et al., 2019). If these air masses are lifted by a trough upstream of the block, the risk of heavy precipitation increases (Lenggenhager and Martius, 2019).

The CMIP6 simulations could simulate the seasonality of heavy precipitation days in Eastern Germany, but overestimated the number of heavy precipitation days during summer in Western Germany. Furthermore, the CMIP6 simulations did not simulate the regional and seasonal differences in the link between blocking and heavy precipitation found in the reanalyses (see Table 5 and Table 6). This is potentially related to the coarse resolution of the models. Mahajan et al. (2015) found an improved representation of stationary (i.e. potentially linked to blocking) heavy precipitation events over the US in climate models with increased spatial resolution. Bador et al. (2020) found increased precipitation amounts in simulations with increased resolution, but resulting in an overestimation of precipitation extremes. They claimed that resolution is not the only key to improve representation of heavy precipitation in climate models. Additionally, the dynamical core and physical parametrisations are reasons for mis-representation of heavy precipitation in climate models which must be improved (Bador et al., 2020). Furthermore, the climate models do not provide hourly precipitation data. Consequently, an analysis based on daily precipitation data was necessary, and it was not possible to distinguish between hourly (i.e. convective) and daily (i.e. large-scale) precipitation events.

For the future, the models simulated only slight changes in the link between blocking and heavy precipitation, but an increase in the total number of heavy precipitation days in both, the summer and the winter half-year. The increase is in accordance with the Clausius-Clapeyron equation which describes an increase of 7% water vapour capacity in the atmosphere per Kelvin resulting in higher potential for heavy precipitation. As described in the results section, the increase in $f_{block|Pr}$ is related to an increased $f_{block|Pr}$ of the CESM2 and NorESM2-MM. In these projections, the blocking frequency increases (Lohmann et al., 2024) which could foster the increase in $f_{block|Pr}$. Changes in the link between blocking and heavy precipitation are hard to estimate because future blocking projections are uncertain (Davini and D'Andrea, 2020; Lohmann et al., 2024) and the ORs have a wide range in the ensemble in the future scenario (Table S11, Table S12, and Fig. 5). Furthermore, the number of heavy precipitation days is small compared to the blocking days. Thus, the statistic is not robust against small changes in the number of blocking or heavy precipitation days.

Calms in Germany were linked to blocking over Central Europe and the North Sea. This location corresponds to the weather pattern "High over Central Europe" which is the most frequent weather pattern during periods with low wind and solar energy production (Drücke et al., 2021). In the winter half-year, the OR was higher than in the summer half-year. The link between blocking and calms during the winter half-year was stronger than with heavy precipitation, but weaker than with heatwaves. The location close to the centre of the block causes weak winds (Grams et al., 2017; Drücke et al., 2021; Mockert et al., 2023). However, weak winds have different sources. One possibility are high-pressure systems which are not stable enough to be counted as blocking, but with the same effect on the wind speed as blocking. Furthermore, calms can occur in low pressure systems or troughs over Central Europe with weak pressure gradients (Drücke et al., 2021), or in saddle points between several pressure systems with weak pressure gradients (Mockert et al., 2023). Weather patterns with weak pressure gradients without

https://doi.org/10.5194/egusphere-2025-3670
Preprint. Discussion started: 19 September 2025

blocking are common in summer resulting in reduced wind energy production during that time of the year (Drücke et al., 2021). This might explain the stronger link between blocking and calms in the winter than in the summer half-year.

The CMIP6 simulations slightly overestimated the link between blocking and calms, but were close to the reanalyses. This indicates that the climate models could simulate the mechanism between blocking and calms in principle. Climate models with low resolution can simulate synoptic-scale winds properly, except over complex terrain like the Alps (Carvalho et al., 2021). During the winter half-year, the simulations underestimated the total number of calm days. Thus, the climate simulations have a seasonal shift in the occurrence of calm days. Despite the underestimation in the total number of calm days in the winter half-year, the climate simulations overestimated the link between blocking and calms.

For the future, the simulations show an increase in the number of calm days and the OR during the winter half-year. The increase in calm days agrees with the projected decrease in the number of days with wind speeds usable for wind turbines (i.e. above the cut-in wind speed and below the cut-off speed, i.e. the speed where the turbine is shut down) (Carvalho et al., 2021). The increase in the OR indicates an increase in the link between blocking and calms, but is not robust, since the ensemble range of the scenario is close to the ensemble range of the historical period (Fig. 5). Unlike temperature and precipitation trends which are influenced by thermodynamics (more heatwaves in a warmer climate and more heavy precipitation due to the Clausius-Clapeyron equation) quite obviously, the occurrence of calms is influenced by weather regimes (Mockert et al., 2023) whose changes are less obvious than changes in thermodynamics.

5 Conclusions

This study investigated the statistical link between blocking and extreme heatwave, heavy precipitation, and calm events in Germany in three reanalyses and six CMIP6 climate simulations using the odds ratio (OR). The study confirms a statistical link between blocking and all three types of extremes found in previous studies (Grams et al., 2017; Kautz et al., 2022). New is the increased robustness of the results as a consequence of the large dataset of three reanalyses and six CMIP6 simulations and the usage of an index which detects the spatial extent of the blocking.

Comparing the ORs of blocking and the three different types of extremes revealed the highest ORs for heatwaves (summer and winter half-year) which were significant at the 5% level. The blocking location differed between summer and winter half-year: in the former time of the year, the blocking centre was Central Europe and in the latter Southern Europe. The different geographical locations between summer and winter are related to different processes driving heatwaves: subsidence and solar insolation in summer, advection of warm air masses in winter. Compared to all heatwaves, the OR of strong heatwaves increased in the summer half-year, but reduced in the winter half-year. The ORs of blocking and heavy precipitation were significant at the 5% level in the summer half-year and blocking locations were Scandinavia and Eastern Europe. In the winter half-year, blocking hampered the occurrence of heavy precipitation (OR<1). Calms were, as heatwaves, linked to blocking over Central Europe. Compared to heatwaves, the average position of the blocks was shifted slightly northward, and the OR was significant only during the winter half-year. Thus, the study shows the statistical significance of blocking on extreme events, especially on heatwaves.

https://doi.org/10.5194/egusphere-2025-3670
Preprint. Discussion started: 19 September 2025

The realisation of the statistical link between blocking and extremes in the CMIP6 simulations depended on the type of extremes. The statistical links between blocking and large-scale events (heatwaves and calms) agreed overall with the reanalyses, but the link between blocking and strong summer heatwaves was underestimated. Furthermore, the ORs of strong heatwaves (summer and winter) have a wide range in the historical simulations. The climate models simulated the seasonality of extremes and the link between blocking and extremes roughly. For example, the seasonality of heavy precipitation events in Eastern Germany was simulated, but not in Western Germany and the link between blocking and heavy precipitation events was underestimated. Low spatial resolution and deficits in the dynamical core and physical parametrisations of the model hamper an accurate representation of heavy precipitation events in climate simulations (Bador et al., 2020). Thus, models have to be improved to have a more reliable representation of heavy precipitation events.

In a future climate assuming the SSP5-8.5 scenario, the number of days with all three types of extremes is projected to increase. Heatwaves are the extreme type with the most pronounced increase in the number of days. Regarding the statistical link between blocking and the three types of extremes, the largest changes were simulated for the link between blocking and heatwaves. The models simulated a robust decrease in $f_{block|HW}$ and a robust increase in $f_{HW|block}$ and $f_{HW|no\ block}$. However, the changes in the ORs of heatwaves are not robust except for all winter heatwaves because the ORs of the scenario simulations are in the historical ensemble range. The projected changes in links between blocking and calms respectively heavy precipitation are moderate and not robust, since the ensemble range of their ORs in the scenario is close to the ensemble range of their ORs in the historical period. Hence, no robust conclusions about changes in the future link between blocking and extreme events are possible. Note that the projected changes in the occurrence of extremes are uncertain. For example, the increase in future summer heatwaves will be damped if blocking decreases. If future blocking increases, the projected increase in heatwaves might be too conservative. Thus, a better representation of blocking in global climate models is necessary to get more robust results regarding future extreme events.

Appendix A: Contingency table

Table A1 shows the four entries in a 2x2 contingency table with respect to the occurrence of extreme events and blocking.

Table A1. Schematic depiction of a contingency table.

		Blocking	
		yes	no
Extreme event	yes	hits	misses
	no	false alarms	correct rejection

https://doi.org/10.5194/egusphere-2025-3670
Preprint. Discussion started: 19 September 2025

Data availability. CMIP6 data are available through https://esgf-data.dkrz.de/search/cmip6-dkrz/, ERA5 data are available through https://climate.copernicus.eu/climate-reanalysis and 20CR are available through https://psl.noaa.gov/data/20thC_Rean/. ERA-20C were downloaded from https://www.ecmwf.int/en/forecasts/dataset/ecmwf-reanalysis-20th-century-using-surface-observations-only, but cannot be downloaded from this URL since ECMWF closed the download service on 1st June 2023.

Author contributions. RL, CP and BA determined the research outline, RL and CP made the data analysis, RL wrote the original draft, CP and BA reviewed the manuscript.

Competing interests. The authors declare no conflict of interest.

Acknowledgements. The authors thank the German States Hesse (grant number 190921020001), Rhineland-Palatinate (grant number 5.4/01/21), Lower Saxony (grant number ZW6-80152457), and Saxony (grant number Z1214/19) for funding this research. Furthermore, the authors thank the German Research Foundation [Deutsche Forschungsgemeinschaft (DFG)] for partially funding this research via the Research Group FOR 2416 "Space-Time Dynamics of Extreme Floods" (SPATE, grant number 278017089), and the European Union for partially funding this research via the project "DevelopIng STratEgies by integrating mitigatioN, aDaptation and participation to climate changE Risks" (DISTENDER, grant number 101056836) from the Horizon EU research and innovation program. The authors thank all groups contributing to CMIP6 for producing and publishing the data, and thank the German Climate Computing Center [Deutsches Klimarechenzentrum (DKRZ)] for providing the data for the CMIP6 simulations on a central platform. Finally, the authors thank the ECMWF for providing the data for ERA5 and ERA-20C and NOAA for the 20CR reanalysis.

https://doi.org/10.5194/egusphere-2025-3670
Preprint. Discussion started: 19 September 2025

References

Andrews, T., Andrews, M. B., Bodas-Salcedo, A., Jones, G. S., Kuhlbrodt, T., Manners, J., Menary, M. B., Ridley, J., Ringer, M. A., Sellar, A. A., Senior, C. A., and Tang, Y.: Forcings, feedbacks, and climate sensitivity in HadGEM3-GC3.1 and UKESM1, J. Adv. Model Earth Sy., 11, 4377–4394, https://doi.org/10.1029/2019MS001866, 2019.

Bador, M., Boé, J., Terray, L., Alexander, L. V., Baker, A., Bellucci, A., Haarsma, R., Koenigk, T., Moine, M., Lohmann, K., Putrasahan, D. A., Roberts, C., Roberts, M., Scoccimarro, E., Schiemann, R., Seddon, J., Senan, R., Valcke, S., and Vanniere, B.: Impact of higher spatial atmospheric resolution on precipitation extremes over land in global climate models, J. Geophys. Res.- Atmos., 125, https://doi.org/10.1029/2019JD032184, 2020.

Bailey, N. T.: Statistical Methods in Biology, Cambridge University Press, ISBN 9781139170840, https://doi.org/https://doi.org/10.1017/CBO9781139170840, 1995.

Barriopedro, D., García-Herrera, R., and Trigo, R. M.: Application of blocking diagnosis methods to General Circulation Models. Part I: a novel detection scheme, Clim. Dynam., 35, 1373–1391, https://doi.org/10.1007/s00382-010-0767-5, 2010.

Barriopedro, D., Fischer, E. M., Luterbacher, J., Trigo, R. M., and García-Herrera, R.: The hot summer of 2010: Redrawing the temperature record map of Europe, Science, 332, 220–224, https://doi.org/10.1126/science.1201224, 2011.

Barriopedro, D., García–Herrera, R., Ordóñez, C., Miralles, D. G., and Salcedo–Sanz, S.: Heat waves: Physical understanding and scientific challenges, Rev. Geophys., https://doi.org/10.1029/2022RG000780, 2023.

Bland, J. M.: Statistics Notes: The odds ratio, BMJ, 320, 1468–1468, https://doi.org/10.1136/bmj.320.7247.1468, 2000.

Blöschl, G., Nester, T., Komma, J., Parajka, J., and Perdigão, R. A. P.: The June 2013 flood in the Upper Danube Basin, and comparisons with the 2002, 1954 and 1899 floods, Hydrol. Earth Syst. Sc., 17, 5197–5212, https://doi.org/10.5194/hess-17-5197-2013, 2013.

Blöschl, G., Kiss, A., Viglione, A., Barriendos, M., Böhm, O., Brázdil, R., Coeur, D., Demarée, G., Llasat, M. C., Macdonald, N., Retsö, D., Roald, L., Schmocker-Fackel, P., Amorim, I., Bělínová, M., Benito, G., Bertolin, C., Camuffo, D., Cornel, D., Doktor, R., Elleder, L., Enzi, S., Garcia, J. C., Glaser, R., Hall, J., Haslinger, K., Hofstätter, M., Komma, J., Limanówka, D., Lun, D., Panin, A., Parajka, J., Petrić, H., Rodrigo, F. S., Rohr, C., Schönbein, J., Schulte, L., Silva, L. P., Toonen, W. H. J., Valent, P., Waser, J., and Wetter, O.: Current European flood-rich period exceptional compared with past 500 years, Nature, 583, https://doi.org/10.1038/s41586-020-2478-3, 2020.

Brunner, L., Schaller, N., Anstey, J., Sillmann, J., and Steiner, A. K.: Dependence of present and future European temperature extremes on the location of atmospheric blocking, Geophys. Res. Lett., 45, 6311–6320, https://doi.org/10.1029/2018GL077837, 2018.

Carvalho, D., Rocha, A., Costoya, X., DeCastro, M., and Gómez-Gesteira, M.: Wind energy resource over Europe under CMIP6 future climate projections: What changes from CMIP5 to CMIP6, Renew. Sust. Energ. Rev., 151, 111 594, https://doi.org/10.1016/j.rser.2021.111594, 2021.

Cattiaux, J., Vautard, R., Cassou, C., Yiou, P., Masson-Delmotte, V., and Codron, F.: Winter 2010 in Europe: A cold extreme in a warming climate, Geophys. Res. Lett., 37, https://doi.org/10.1029/2010GL044613, 2010.

Davini, P. and D'Andrea, F.: From CMIP3 to CMIP6: Northern Hemisphere atmospheric blocking simulation in present and future climate, J. Climate, 33, 10 021–10 038, https://doi.org/10.1175/JCLI-D-19-0862.1, 2020.

Davini, P., Cagnazzo, C., Gualdi, S., and Navarra, A.: Bidimensional diagnostics, variability, and trends of Northern Hemisphere blocking, J. Climate, 25, 6496–6509, https://doi.org/10.1175/JCLI-D-12-00032.1, 2012.

https://doi.org/10.5194/egusphere-2025-3670
Preprint. Discussion started: 19 September 2025

Dong, Y., Armour, K. C., Zelinka, M. D., Proistosescu, C., Battisti, D. S., Zhou, C., and Andrews, T.: Intermodel spread in the pattern effect and its contribution to climate sensitivity in CMIP5 and CMIP6 models, J. Climate, 33, 7755–7775, https://doi.org/10.1175/JCLI-D-19-1011.1, 2020.

Drücke, J., Borsche, M., James, P., Kaspar, F., Pfeifroth, U., Ahrens, B., and Trentmann, J.: Climatological analysis of solar and wind energy in Germany using the Grosswetterlagen classification, Renew. Energ., 164, 1254–1266, https://doi.org/10.1016/j.renene.2020.10.102, 2021.

Enercon: ENERCON Wind Turbines, https://www.enercon.de/en/wind-turbines/product-portfolio, last access 24.7.2025, 2025.

Eyring, V., Bony, S., Meehl, G. A., Senior, C. A., Stevens, B., Stouffer, R. J., and Taylor, K. E.: Overview of the Coupled Model Intercomparison Project Phase 6 (CMIP6) experimental design and organization, Geosci. Model Dev., 9, 1937–1958, https://doi.org/10.5194/gmd-9-1937-2016, 2016.

Fischer, E. M., Seneviratne, S. I., Vidale, P. L., Lüthi, D., and Schär, C.: Soil moisture–atmosphere interactions during the 2003 European summer heat wave, J. Climate, 20, 5081–5099, https://doi.org/10.1175/JCLI4288.1, 2007.

Grams, C. M., Binder, H., Pfahl, S., Piaget, N., and Wernli, H.: Atmospheric processes triggering the central European floods in June 2013, Nat. Hazards Earth Syst. Sci., 14, 1691–1702, https://doi.org/10.5194/nhess-14-1691-2014, 2014.

Grams, C. M., Beerli, R., Pfenninger, S., Staffell, I., and Wernli, H.: Balancing Europe's wind-power output through spatial deployment informed by weather regimes, Nat. Clim. Change, 7, 557–562, https://doi.org/10.1038/nclimate3338, 2017.

Hersbach, H., Bell, W., Berrisford, P., Horányi, A., Sabater, J.-M., Nicolas, J., Radu, R., Schepers, D., Simmons, A., Soci, C., and Dee, D.: Global reanalysis: goodbye ERA-Interim, hello ERA5, ECMWF Newsletter, pp. 17–24, https://www.ecmwf.int/en/elibrary/19027-global-reanalysis-goodbye-era-interim-hello-era5, 2019.

Hofstätter, M., Lexer, A., Homann, M., and Blöschl, G.: Large-scale heavy precipitation over central Europe and the role of atmospheric cyclone track types, Int. J. Climatol., 38, https://doi.org/10.1002/joc.5386, 2018.

Holmberg, E., Messori, G., Caballero, R., and Faranda, D.: The link between European warm-temperature extremes and atmospheric persistence, Earth Syst. Dynam., 14, 737–765, https://doi.org/10.5194/esd-14-737-2023, 2023.

Huo, R., Li, L., Chen, H., Xu, C.-Y., Chen, J., and Guo, S.: Extreme precipitation changes in Europe from the last millennium to the end of the twenty-first century, J. Climate, 34, 567–588, https://doi.org/10.1175/JCLI-D-19-0879.1, 2021.

Kadow, C., Illing, S., Lucio-Eceiza, E. E., Bergemann, M., Ramadoss, M., Sommer, P. S., Kunst, O., Schartner, T., Pankatz, K., Grieger, J., Schuster, M., Richling, A., Thiemann, H., Kirchner, I., Rust, H. W., Ludwig, T., Cubasch, U., and Ulbrich, U.: Introduction to Freva – a Free Evaluation System Framework for earth system modeling, J. Open Res. Software, 9, 13, https://doi.org/10.5334/jors.253, 2021.

Kautz, L.-A., Martius, O., Pfahl, S., Pinto, J. G., Ramos, A. M., Sousa, P. M., and Woollings, T.: Atmospheric blocking and weather extremes over the Euro-Atlantic sector – a review, Weather Clim. Dynam., 3, 305–336, https://doi.org/10.5194/wcd-3-305-2022, 2022.

Kovats, R. S. and Kristie, L. E.: Heatwaves and public health in Europe, Eur. J. Public Health, 16, 592–599, https://doi.org/10.1093/eurpub/ckl049, 2006.

Kron, W., Löw, P., and Kundzewicz, Z. W.: Changes in risk of extreme weather events in Europe, Environ. Sci. Policy, 100, 74–83, https://doi.org/10.1016/j.envsci.2019.06.007, 2019.

Lehmann, J. and Coumou, D.: The influence of mid-latitude storm tracks on hot, cold, dry and wet extremes, Sci. Rep., 5, 17 491, https://doi.org/10.1038/srep17491, 2015.

Lenggenhager, S. and Martius, O.: Atmospheric blocks modulate the odds of heavy precipitation events in Europe, Clim. Dynam., 53, 4155–4171, https://doi.org/10.1007/s00382-019-04779-0, 2019.

https://doi.org/10.5194/egusphere-2025-3670
Preprint. Discussion started: 19 September 2025

Lin, C., Kjellström, E., Wilcke, R. A. I., and Chen, D.: Present and future European heat wave magnitudes: climatologies, trends, and their associated uncertainties in GCM-RCM model chains, Earth Syst. Dynam., 13, 1197–1214, https://doi.org/10.5194/esd-13-1197-2022, 2022.

Lohmann, R., Purr, C., and Ahrens, B.: Northern Hemisphere atmospheric blocking in CMIP6 climate projections using a hybrid index, J. Climate, https://doi.org/https://doi.org/10.1175/JCLI-D-23-0589.1, 2024.

Mahajan, S., Evans, K. J., Branstetter, M., Anantharaj, V., and Leifeld, J. K.: Fidelity of precipitation extremes in high resolution global climate simulations, Procedia Comput. Sci., 51, 2178–2187, https://doi.org/10.1016/j.procs.2015.05.492, 2015.

Miralles, D. G., Teuling, A. J., van Heerwaarden, C. C., and Vilà-Guerau de Arellano, J.: Mega-heatwave temperatures due to combined soil desiccation and atmospheric heat accumulation, Nat. Geosci., 7, 345–349, https://doi.org/10.1038/ngeo2141, 2014.

Mockert, F., Grams, C. M., Brown, T., and Neumann, F.: Meteorological conditions during periods of low wind speed and insolation in Germany: The role of weather regimes, Meteorol. Appl., 30, https://doi.org/10.1002/met.2141, 2023.

Mohr, S., Wandel, J., Lenggenhager, S., and Martius, O.: Relationship between atmospheric blocking and warm-season thunderstorms over western and central Europe, Q. J. Roy. Meteor. Soc., 145, 3040–3056, https://doi.org/10.1002/qj.3603, 2019.

Pfahl, S.: Characterising the relationship between weather extremes in Europe and synoptic circulation features, Nat. Hazards Earth Syst. Sci., 14, https://doi.org/10.5194/nhess-14-1461-2014, 2014.

Pfahl, S. and Wernli, H.: Quantifying the relevance of atmospheric blocking for co-located temperature extremes in the Northern Hemisphere on (sub-)daily time scales, Geophys. Res. Lett., 39, https://doi.org/10.1029/2012GL052261, 2012.

Poli, P., Hersbach, H., Dee, D. P., Berrisford, P., Simmons, A. J., Vitart, F., Laloyaux, P., Tan, D. G. H., Peubey, C., Thépaut, J.-N., Trémolet, Y., Hólm, E. V., Bonavita, M., Isaksen, L., and Fisher, M.: ERA-20C: An atmospheric reanalysis of the twentieth century, J. Climate, 29, 4083–4097, https://doi.org/10.1175/JCLI-D-15-0556.1, 2016.

Priestley, M. D. K., Ackerley, D., Catto, J. L., Hodges, K. I., McDonald, R. E., and Lee, R. W.: An overview of the extratropical storm tracks in CMIP6 historical simulations, J. Climate, 33, 6315–6343, https://doi.org/10.1175/JCLI-D-19-0928.1, 2020.

R Core Team: R: A language and environment for statistical computing, R Foundation for Statistical Computing, Vienna, Austria, https://www.R-project.org/, 2024.

Raška, P.: Flood risk perception in Central-Eastern European members states of the EU: a review, Nat. Hazards, 79, 2163–2179, https://doi.org/10.1007/s11069-015-1929-x, 2015.

Rex, D. F.: Blocking action in the middle troposphere and its effect upon regional climate, Tellus, 2, 196–211, https://www.tandfonline.com/doi/abs/10.3402/tellusa.v2i3.8546, 1950.

Richling, A.: 2D-Blocking, Tech. rep., FU Berlin, https://gitlab.met.fu-berlin.de/tools4freva/blocking_2D, 2020.

Russo, S., Dosio, A., Graversen, R. G., Sillmann, J., Carrao, H., Dunbar, M. B., Singleton, A., Montagna, P., Barbola, P., and Vogt, J. V.: Magnitude of extreme heat waves in present climate and their projection in a warming world, J. Geophys. Res.- Atmos., 119, https://doi.org/10.1002/2014JD022098, 2014.

Russo, S., Sillmann, J., and Fischer, E. M.: Top ten European heatwaves since 1950 and their occurrence in the coming decades, Environ. Res. Lett., 10, 124 003, https://doi.org/10.1088/1748-9326/10/12/124003, 2015.

Ruxton, G. D. and Neuhäuser, M.: Good practice in testing for an association in contingency tables, Behav. Ecol. Sociobiol., 64, 1505–1513, https://doi.org/10.1007/s00265-010-1014-0, 2010.

Ruxton, G. D. and Neuhäuser, M.: Review of alternative approaches to calculation of a confidence interval for the odds ratio of a 2 × 2 contingency table, Methods Ecol. Evol., 4, 9–13, https://doi.org/10.1111/j.2041-210x.2012.00250.x, 2013.

https://doi.org/10.5194/egusphere-2025-3670
Preprint. Discussion started: 19 September 2025

Schaller, N., Sillmann, J., Anstey, J., Fischer, E. M., Grams, C. M., and Russo, S.: Influence of blocking on Northern European and Western Russian heatwaves in large climate model ensembles, Environ. Res. Lett., 13, 054 015, https://doi.org/10.1088/1748-9326/aaba55, 2018.

Sillmann, J. and Croci-Maspoli, M.: Present and future atmospheric blocking and its impact on European mean and extreme climate, Geophys. Res. Lett., 36, https://doi.org/10.1029/2009GL038259, 2009.

Sillmann, J., Croci-Maspoli, M., Kallache, M., and Katz, R. W.: Extreme cold winter temperatures in Europe under the influence of North Atlantic atmospheric blocking, J. Climate, 24, 5899–5913, https://doi.org/10.1175/2011JCLI4075.1, 2011.

Slivinski, L. C., Compo, G. P., Whitaker, J. S., Sardeshmukh, P. D., Giese, B. S., McColl, C., Allan, R., Yin, X., Vose, R., Titchner, H., Kennedy, J., Spencer, L. J., Ashcroft, L., Brönnimann, S., Brunet, M., Camuffo, D., Cornes, R., Cram, T. A., Crouthamel, R., Domínguez-Castro, F., Freeman, J. E., Gergis, J., Hawkins, E., Jones, P. D., Jourdain, S., Kaplan, A., Kubota, H., Blancq, F. L., Lee, T., Lorrey, A., Luterbacher, J., Maugeri, M., Mock, C. J., Moore, G. K., Przybylak, R., Pudmenzky, C., Reason, C., Slonosky, V. C., Smith, C. A., Tinz, B., Trewin, B., Valente, M. A., Wang, X. L., Wilkinson, C., Wood, K., and Wyszyński, P.: Towards a more reliable historical reanalysis: Improvements for version 3 of the Twentieth Century Reanalysis system, Q. J. Roy. Meteor. Soc., 145, 2876–2908, https://doi.org/10.1002/qj.3598, 2019.

Sousa, P. M., Trigo, R. M., Barriopedro, D., Soares, P. M. M., Ramos, A. M., and Liberato, M. L. R.: Responses of European precipitation distributions and regimes to different blocking locations, Clim. Dynam., 48, 1141–1160, https://doi.org/10.1007/s00382-016-3132-5, 2017.

Sousa, P. M., Trigo, R. M., Barriopedro, D., Soares, P. M. M., and Santos, J. A.: European temperature responses to blocking and ridge regional patterns, Clim. Dynam., 50, 457–477, https://doi.org/10.1007/s00382-017-3620-2, 2018.

Stanley, K., Leps, N., Hänsel, S., Klippel, L., Imbery, F., and Walter, A.: Recent hot and dry summers in Germany in comparison to climate projections, Meteorol. Z., 32, 113–142, https://doi.org/10.1127/metz/2022/1152, 2023.

Stephenson, D. B.: Use of the "odds ratio" for diagnosing forecast skill, Weather Forecast., 15, 221–232, https://doi.org/10.1175/1520-0434(2000)015<0221:UOTORF>2.0.CO;2, 2000.

Suarez-Gutierrez, L., Müller, W. A., Li, C., and Marotzke, J.: Dynamical and thermodynamical drivers of variability in European summer heat extremes, Clim. Dynam., 54, https://doi.org/10.1007/s00382-020-05233-2, 2020.

Tradowsky, J. S., Philip, S. Y., Kreienkamp, F., Kew, S. F., Lorenz, P., Arrighi, J., Bettmann, T., Caluwaerts, S., Chan, S. C., De Cruz, L., de Vries, H., Demuth, N., Ferrone, A., Fischer, E. M., Fowler, H. J., Goergen, K., Heinrich, D., Henrichs, Y., Kaspar, F., Lenderink, G., Nilson, E., Otto, F. E. L., Ragone, F., Seneviratne, S. I., Singh, R. K., Skålevåg, A., Termonia, P., Thalheimer, L., van Aalst, M., Van den Bergh, J., Van de Vyver, H., Vannitsem, S., van Oldenborgh, G. J., Van Schaeybroeck, B., Vautard, R., Vonk, D., and Wanders, N.: Attribution of the heavy rainfall events leading to severe flooding in Western Europe during July 2021, Climatic Change, 176, 90, https://doi.org/10.1007/s10584-023-03502-7, 2023.

Tuel, A. and Martius, O.: Persistent warm and cold spells in the Northern Hemisphere extratropics: regionalisation, synoptic-scale dynamics and temperature budget, Weather Clim. Dynam., 5, 263–292, https://doi.org/10.5194/wcd-5-263-2024, 2024.

Woollings, T., Barriopedro, D., Methven, J., Son, S.-W., Martius, O., Harvey, B., Sillmann, J., Lupo, A. R., and Seneviratne, S.: Blocking and its response to climate change, Curr. Clim. Change Rep., 4, 287–300, https://doi.org/10.1007/s40641-018-0108-z, 2018.

Yao, Y. and De-Hai, L.: The anomalous European climates linked to different Euro-Atlantic blocking, Atmos. Oceanic Sci. Lett., 7, 309–313, https://doi.org/https://doi.org/10.3878/j.issn.1674-2834.14.0001, 2014.

Zampieri, M., Ceglar, A., Dentener, F., and Toreti, A.: Wheat yield loss attributable to heat waves, drought and water excess at the global, national and subnational scales, Environ. Res. Lett., 12, 064 008, https://doi.org/10.1088/1748-9326/aa723b, 2017.

https://doi.org/10.5194/egusphere-2025-3670
Preprint. Discussion started: 19 September 2025

Zschenderlein, P., Fink, A. H., Pfahl, S., and Wernli, H.: Processes determining heat waves across different European climates, Q. J. Roy. Meteor. Soc., 145, 2973–2989, https://doi.org/10.1002/qj.3599, 2019.